

P. MYŚLIWIEC¹, R.E. ŚLIWA^{1*}, R. OSTROWSKI¹, M. BUJNY², M. ZWOLAK¹**EFFECT OF WELDING PARAMETERS AND METAL ARRANGEMENT OF THE AA2024-T3 ON THE QUALITY AND STRENGTH OF FSW LAP JOINTS FOR JOINING ELEMENTS OF LANDING GEAR BEAM**

The paper presents the possibility of using FSW technology for joining elements of a landing gear beam of the M28 aircraft. The FSW process was performed on a 4-axis numerical machine under industrial conditions. However, before welding was carried out under industrial conditions, preliminary experimental tests were carried out under laboratory conditions. Preliminary research was carried out for AA2024-T3 aluminum sheets of 1 mm and 3 mm in thickness, joined in a lap configuration. The influence of technological and geometric parameters of the process on the quality and strength of the weld was examined. Sheet metal arrangement was analyzed. Tests were carried out for two configurations. The first of which with 1 mm sheet on the top and 3 mm sheet on the bottom and in reverse order. It has been shown that setting a thicker plate on the top gives a 40% better strength. The microhardness and microstructure of the weld were tested. During the laboratory tests, low-cycle fatigue tests of the FSW lap joint were performed. It has been shown that the FSW method can be an alternative to the riveting process in the production of aviation structure elements.

Keywords: FSW lap joints, aluminum alloys, landing gear beam, low cycle fatigue test

1. Introduction

Since the invention of friction stir welding, by TWI in 1991 [1], significant advances have been reached within materials, tools, parameter optimization, process control, as well as, a better understanding of the process itself. This has led to an increased number of applications in different industrial areas, including the automotive industry. Other areas of application include marine, railway and aerospace industries which explore and use FSW due to its great advantages of distortion and mechanical properties when compared with other techniques, as well as, its ability to weld “unweldable” aluminum alloys [2]. Fig. 1. shows a lap joint for illustration, other types of joints such as butt joints and fillet joints can also be fabricated by FSW.

FSW technique has numerous advantages over traditional welding practices. FSW joints possess sufficiently high strength, approximately equal to the strength of original material. Considerable weight reduction is possible by the implementation of this technique. It is possible to join alloys that cannot be welded feasibly with the help of fusion welding methods. FSW is executed at a temperature beneath the base metal’s melting point [3,4]. Thus, all anomalies pertaining to re-solidification of welded material, like porosity, brittleness and crack genera-

tion can be avoided [5,6]. As the FSW process is carried out at lower temperatures, it does not experience much distortion and residual stresses. This technique also imparts great dimensional stability. Unlike the conventional welding processes, FSW does not require any filler material or shielding gas [7,8]. Due to innumerable qualities and advantages of FSW over conventional joining processes, it has become a rapidly emerging solid-state joining method [9].

The main purpose of the presented work is to manufacture the front landing gear beam of the M28 aircraft shown in Figure 2, using FSW technology. The whole assembly consists of two elements in a mirror image, which are currently joined by riveting technology. All components of the assembly are made of AA2024-T3 aluminum alloy. The thickness of the joined elements is in the range of 1 mm to 3 mm. A preliminary study was the first stage of work. The influence of technological and geometric parameters of the process on the quality of FSW joints was analyzed. Overlapping joints with 3-1 and 1-3 arrangement were tested. Marking 3-1 shows the situation where the 3 mm plate is at the top from the tool side and the plate 1 mm at the bottom. Marks 1-3 show the reverse arrangement. The quality of joints was determined on the basis of a static tensile test. Then, for selected joints, microhardness measurement and microstructure

¹ RZESZOW UNIVERSITY OF TECHNOLOGY, 12 POWSTAŃCÓW WARSZAWY AV, 35-959 RZESZÓW, POLAND

² ULTRATECH SP. Z.O.O, 4A FABRYCZNA RD. 39-120 SEDZISZÓW MLP. POLAND

* Corresponding author: rslwiwa@prz.edu.pl



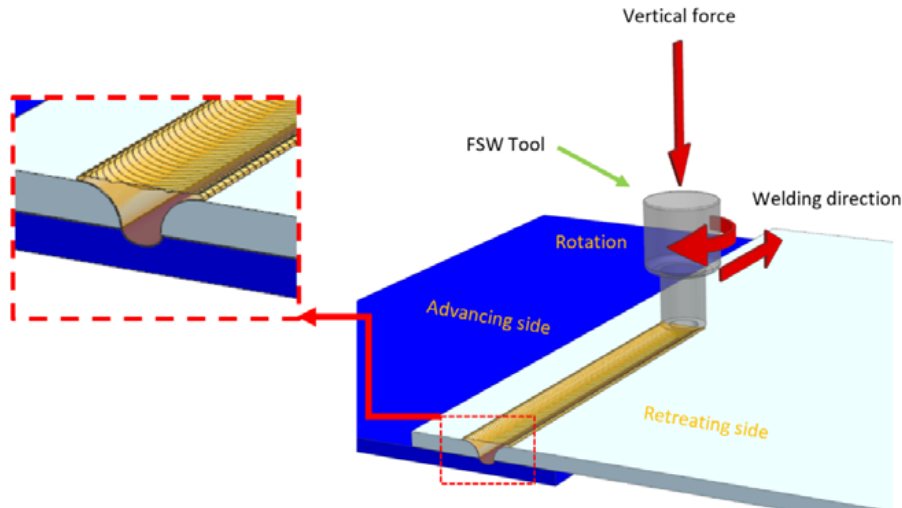


Fig. 1. Scheme of the FSW process – a lap joint

analysis were performed. The joint with the best mechanical properties was subjected to a low-cycle fatigue test.

In the second stage, having acquired experience in the field of FSW and test results from the first stage, the landing gear beam of the M28 aircraft was made. It has been shown that it is possible to implement FSW technology for the production of parts of the aviation structure. Thus, the use of FSW technology has eliminated riveted connections as it has so far.

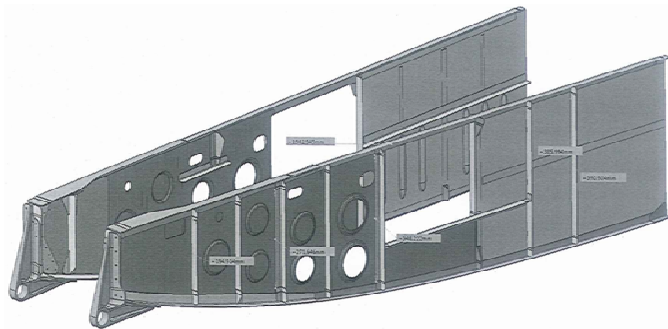


Fig. 2. The view of a landing gear beam assembly of the M28 aircraft (elements are in the range of 1 mm to 3 mm in thickness)

2. Experimental procedure

To perform the preliminary study a cold rolled sheet of AA2024-T3 of 1 mm and 3 mm in thickness was used. The 3 mm sheet was covered with a layer of Al-clad. In this investigation, the joining region was carefully cleaned prior to welding, but the oxides could not be removed thoroughly. After being polished by abrasive paper and cleaned with acetone, several weld plates were subjected to FSW along the rolling direction. The blank sheet dimensions were 180×100 mm. A backing plate with two holders constituted the fixture to firmly hold the workpiece. A fixing device with the workpiece were installed on the plate of piezoelectric Kistler dynamometer shown in Fig. 3a. The FSW experiments were carried out on a specially adopted CNC milling machine (Fig. 3b) using the welding tool shown in Fig. 4.

Tools with a tapered threaded pin and a shoulder with spiral grooves were used. Depending on the configuration, two tool sizes were used, shown in Figure 4. The tool diameter was 15 mm and 12 mm. Both tools were produced from high-speed steel. Tool dimension was adjusted to the material sheet thickness according to the algorithm shown in literature [10]. Tool

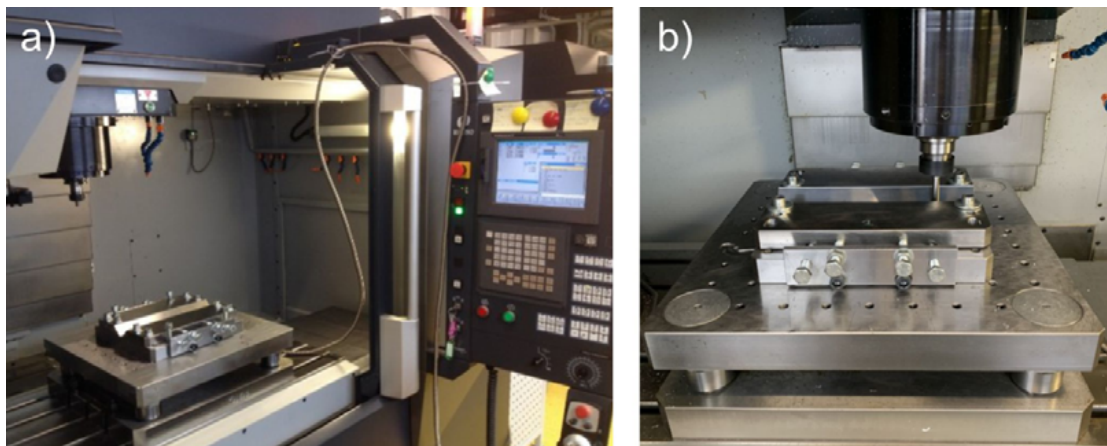


Fig. 3. a) General view of 3-axis CNC machine (Makino PS 95) adopted for FSW process, b) View of mounting device used in FSW process installed on dynamometer plate

dimensions were determined according to the following relationships: \varnothing shoulder: $\sim 2,2 \times \text{mat. thick.} + 7,3$, \varnothing pin: $\sim 0,8 \times \text{mat. thick.} + 2,2$. Generally we can assume that the ratio of shoulder diameter to pin diameter is around 3. Tool worked without a tilt angle, perpendicular to the surface of the welded material [11].

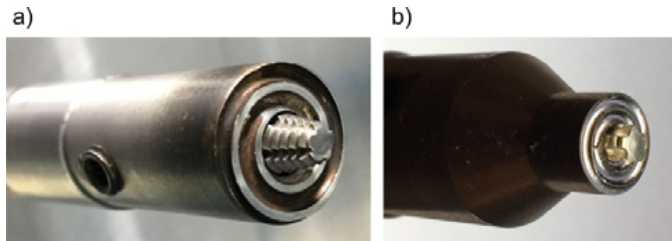


Fig. 4. FSW tool dimension, a) 15 mm in diameter., b) 12 mm in diameter

The lap joint configuration was prepared to produce the joints. Welding has been done on the 180 mm long section. Two configurations of sheet metal arrangement were analyzed. The first configuration where a 3 mm plate was placed on the top and the second one where a 1 mm plate was placed on the top. This is schematically shown in Figure 5.

The technological parameters of the welding process, axial forces acting on the tool and the load capacity of the lap joints for both arrangement configurations are shown in Table 1 and 2. The resulting FSW joints are shown in Table 3 and 4, respectively for both configurations. FSW joint quality depends mainly on the heat produced during the process to create appropriate conditions for the correct flow of the plasticized material. Of course, this state is influenced by the process input parameters

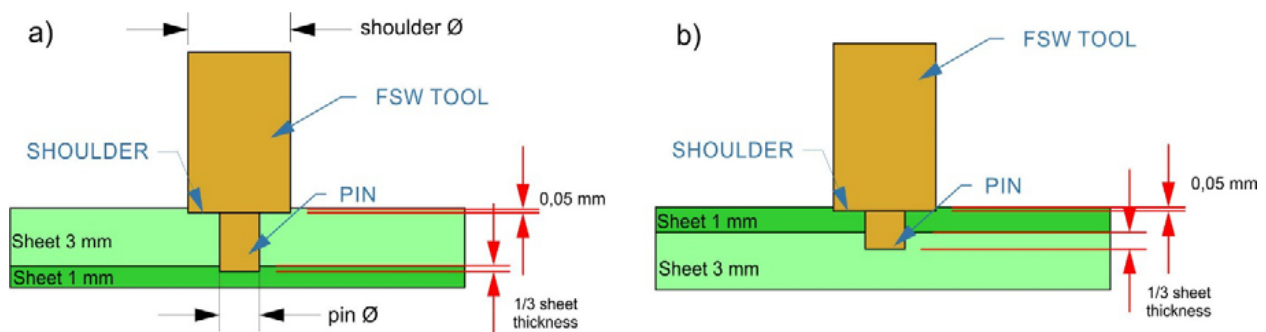


Fig. 5. Scheme of sheet metal configurations and FSW tool, a) sheets 3 mm and 1 mm: set 3-1, b) sheets 1 mm and 3 mm: set 1-3

TABLE 1

Technological parameters and properties of lap joints of 3 mm and 1 mm in thickness of AA 2024-T3 sheets obtained by linear FSW process

Weld No.	Technological parameters [rpm]/[mm/min] ω/v	Weld pitch ω/v	Weld capacity [N]	Joint effectiveness [%]	Max welding force (in Z axis) $F_{z \max}$ [N]	Average welding force (in Z axis) [N]
2	900 / 200	0,22	14276	66	13495	9785
5	900 / 250	0,28	11248	52	15157	10773
1	800 / 250	0,31	18886	87	15055	10191
4	700 / 200	0,29	18048	83	13861	9403
6	700 / 150	0,21	18628	86	13941	9881
3	800 / 200	0,25	19046	88	14177	10651
7	600 / 150	0,25	18109	84	15640	11479
	Parent material		21630			

TABLE 2

Technological parameters and properties of lap joints of 1 mm and 3 mm in thickness of AA 2024-T3 sheets obtained by linear FSW process

Weld No.	Technological parameters [rpm]/[mm/min] ω/v	Weld pitch ω/v	Weld capacity [N]	Joint effectiveness [%]	Max welding force (in Z axis) $F_{z \max}$ [N]	Average welding force (in Z axis) [N]
2	900 / 200	0,22	7127,5	33	7854	4602
5	900 / 250	0,28	7575	35	7449	4734
1	800 / 250	0,31	5557,5	26	7305	4756
4	700 / 200	0,29	2407,5	11	8769	5527
6	700 / 150	0,21	11350	52	9018	6129
3	800/200	0,25	10275	48	8380	6226
7	600/150	0,25	10975	51	8032	6330

discussed above, i.e. the rotational speed of the tool, welding speed and axial force acting on the tool which is determined by the depth of immersion of the tool. Typically, high welding speeds generate low heat from friction, while high speed tool/spindle generates a lot of heat during the FSW process. In addition, excessive axial force is responsible for generating large amounts of heat and vice versa. In friction stir welding, all three parameters work together and affect the weld strength. The range of technological parameters was determined empirically on the basis of pilot studies. Many tests were carried out with different technological parameters. Too “cold parameters” result in an inadequate level of plasticity of the joined materials and the

formation of discontinuities in the weld. Too “hot parameters” cause local melting, which negatively affects the weld strength.

2.1. Tensile testing of FSW joints

The obtained FSW joints were the basis to make specimens for tensile tests and metallographic examinations. The mechanical properties of the joints were measured during tensile testing, as well as micro hardness testing. Tensile specimens dimensions are shown in Fig. 6. Specimen preparation was performed using wire EDM machining.

TABLE 3

Views of FSW lap joints of 1 mm and 3 mm AA2024-T3 sheets





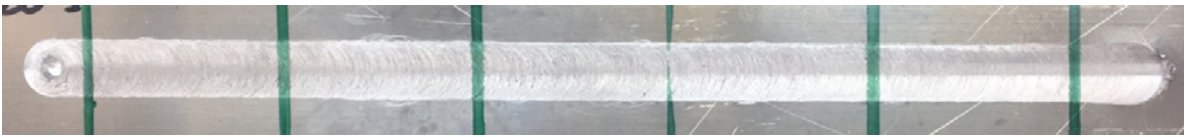




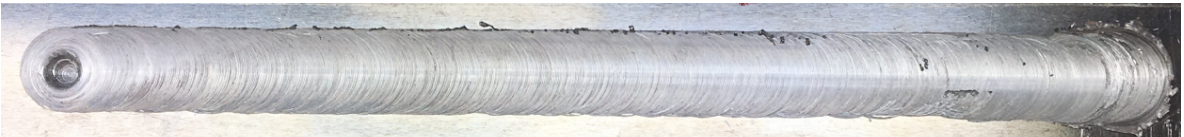




	Rotational speed [rpm]/ welding speed [mm/min]	View of the FSW lap joints from the face side
1	800 [rpm]/250 [mm/min]	
2	900 [rpm]/200 [mm/min]	
3	800 [rpm]/200 [mm/min]	
4	700 [rpm]/200 [mm/min]	
5	900 [rpm]/250 [mm/min]	
6	700 [rpm]/150 [mm/min]	
7	600 [rpm]/150 [mm/min]	

TABLE 4

Views of FSW lap joints of 3 mm and 1 mm AA2024-T3 sheets

	Rotational speed [rpm]/ welding speed [mm/min]	View of the FSW lap joints from the face side
1	800 [rpm]/250 [mm/min]	
2	900 [rpm]/200 [mm/min]	
3	800 [rpm]/200 [mm/min]	
4	700 [rpm]/200 [mm/min]	
5	900 [rpm]/250 [mm/min]	
6	700 [rpm]/150 [mm/min]	
7	600 [rpm]/150 [mm/min]	

The tensile tests were carried out on a Zwick/Roell Z 100 universal testing machine, at room temperature. An extensometer with a gauge length of $L_0 = 50$ mm was used for strain data acquisition. The results, given by the average braking force of FSW joints were obtained by uniaxial tensile test. Mechanical properties of FSW joints were grouped in the Table 1 and 2. The tensile properties of the joints are slightly affected by the rotational and welding speeds and the arrangement of sheets. A comparison of joint load capacity depending on their arrangement is shown

in Figure 7. It can be clearly seen that the arrangement where the thicker sheet is on the top of the fold gives definitely better strength properties than in the case when the thinner sheet is placed at the top of the fold. Differences in strength are even several times higher as shown in Figure 7. A characteristic feature of welding from the thicker side of the sheet is also the low sensitivity of the process and joint quality to changes in technological parameters of the process. The strength of all joints was very similar. It looks much different when welding from the thinner side.

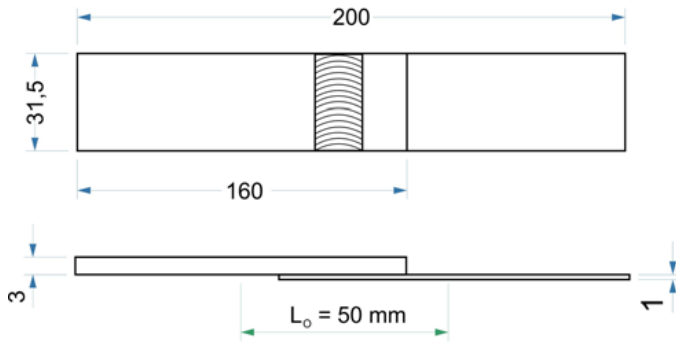


Fig. 6. Geometry of tensile-shear specimen

The impact of technological parameter values is significant. This comparison clearly shows that the implementation of the FSW overlap process from the point of view of the strength of the joint is most preferably carried out from the side of the thicker sheet. An additional advantage of this approach is the stiffer fastening of the sheets, which allows some simplification of the method of fastening the tooling elements. However, the disadvantage of this approach is the creation of a larger axial force acting on the tools and a greater tendency to deform the welded element due to the increase in the amount of heat generated in the process. The reduction of axial force in the FSW process can be achieved by using a tool with a concave shoulder, however, such a tool must work with tilt angle between 1-3°.

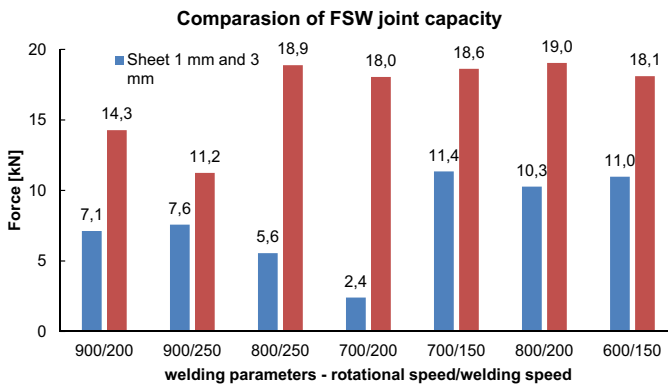


Fig. 7. Comparison of the load capacity of the FSW lap joints depending on the method of arranging the sheets as a function of technological process parameters (rotational speed/welding speed), [sheets 1 and 3, sheets 3 and 1 – explanation in Fig. 5]

2.2. Low cycle fatigue test

Low cycle fatigue has two fundamental characteristics: plastic deformation in each cycle; and low cycle phenomenon, in which the materials have finite endurance for this type of load. The range of low-cycle fatigue compared to the range of high-cycle fatigue differs primarily in the magnitude of plastic deformation. Fatigue analysis of FSW lap joints is often based on experimental results from test specimens. Various standard and nonstandard specimens have been used, but the most common specimen type is the tensile-shear specimen (Fig. 6). The

tensile-shear specimen consists of two overlapping strips of sheet metal joined by FSW technique. Tensile load is applied to the ends of the sheet, nominally placing the weld surface between the sheets in shear. Tensile-shear specimens are used for both strength testing and fatigue testing of FSW lap welds. Fatigue testing is often conducted in the load-controlled, constant-amplitude loading mode with R-ratios greater, lower or equal zero (Fig. 8). The stress ratio, R, is an important parameter and is defined as the algebraic ratio of the minimum to maximum cyclic stresses. R is widely used to distinguish different constant amplitude cyclic loading conditions in fatigue analysis. Data from fatigue tests of these specimens are often presented in the form of load-life data, in which the abscissa is either load amplitude or maximum load [12].

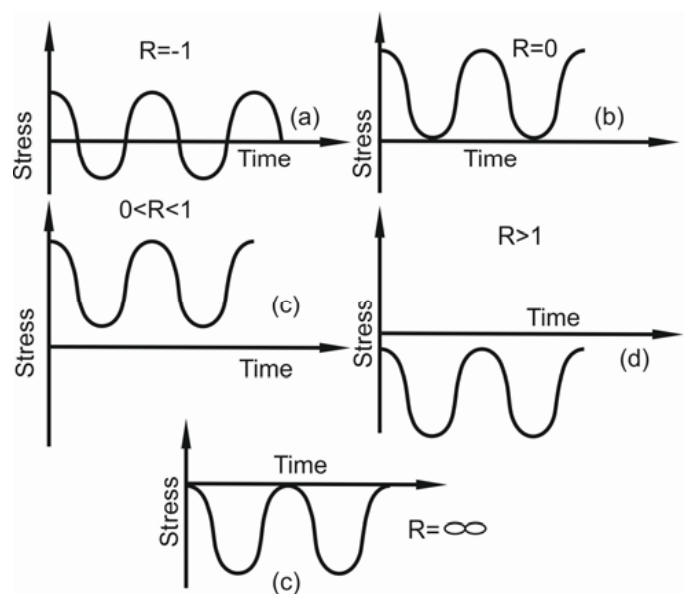


Fig. 8. Typical constant amplitude loading cycles [12]

In order to verify the quality of the FSW weld, low-cycle fatigue tests were carried out on a Zwick/Roell Z100 testing machine at frequency 0.3 Hz. Such a low frequency, characteristic of low cycle tests, allows to avoid heating of samples at heavy loads to be avoided. Six samples were prepared with the dimensions shown in Figure 6. The maximum force required to destroy the sample of a FSW joint in uniaxial tensile test was determined. It was 13700 N. Fatigue tests (cyclic stretching and return to neutral – zero-pulsating, $R = 0$) were performed successively for the data shown in Table 5. During the first test, i.e. determining the maximum breaking force of the FSW joint, the sample broke on the sheet metal side 1 mm thick (on the thinner side). The remaining samples were subjected to a changing load from zero pulsating at a speed of 20 mm/min which corresponded to strain rates equal 6.7×10^{-3} 1/s. In this case the strain rate was calculated as the ratio of traverse speed and gauge length. Table 5 grouped the loading conditions of the samples and the corresponding number of cycles performed until breaking.

Analyzing the results of low-cycle fatigue tests, it can be stated that the geometry of the joint plays a significant role in

strength. During an uniaxial tensile test, where the maximum weld load capacity of the FSW joint was determined, thinner sheet was destroyed – such results were expected. The break occurred outside the weld area. It can therefore be concluded that the strength of the joint is greater than the strength of the thinner sheet. Thus, the large plastic deformation of the material in the FSW process resulted in increased strength of the material at the weld site. The critical place here is the heat affected zone where the microstructure of the material has changed as a result of the increased temperature. This place can be called the so-called structural notch. However, the situation changes dramatically under the influence of dynamic stresses even much lower than the maximum weld load capacity. Here, crack propagation was initiated on the inside of the thick sheet. This is influenced by the geometry of the lap joint and the fact that the nugget zone (NZ) has a lower hardness than the parent material (PM). Gradual load reduction only increased the number of cycles, however the nature of sample destruction has not changed. The 40% of R_m load has changed this. In this case, the thin sheet was damaged. The deflection of thick sheet metal was not so intense thus the thinnest joint element was broken. The summary of results for the low-cycle fatigue test is shown in Table 5 and Figure 9.

TABLE 5

Low-cycle fatigue test data

Test No.	Percentage of static load capacity [%]	Force [N]	Number of cycles
1	100	13700	1
2	80	10960	336
3	70	9590	718
4	60	8220	1714
5	50	6850	3601
6	40	5480	9603

2.3. Macro and microstructure tests

The macro and microstructure analysis was performed for a sample that had the best strength properties of all welds made. It was weld no. 3 (3 mm and 1 mm) made with following tech-

nological parameters: 800 rpm and 200 mm/min. The method of sample preparation is shown in Figure 10.

Figure 11 shows the macrostructure of the FSW weld shown in Figure 10 made with following technological parameters: 800 rpm and 200 mm / min. In cross-section, the weld is characterized by high heterogeneity. From the advancing side the flow lines are very intense, their arrangement indicates a significant degree of deformation while from the retreating side the flowing lines are practically invisible. The surface layer covered with a layer of Al-clad was mixed with the sheet material only in the area strongly plastically deformed (from the advancing side), while on the opposite side the Al-clad layer is almost intact. The phenomenon of complete mixing of the material of welded sheets occurs mainly in the area of 3 mm thick sheet metal, in 1 mm thick sheet metal welding effects take only 1/10 of its cross-section. Along the axis of the weld,

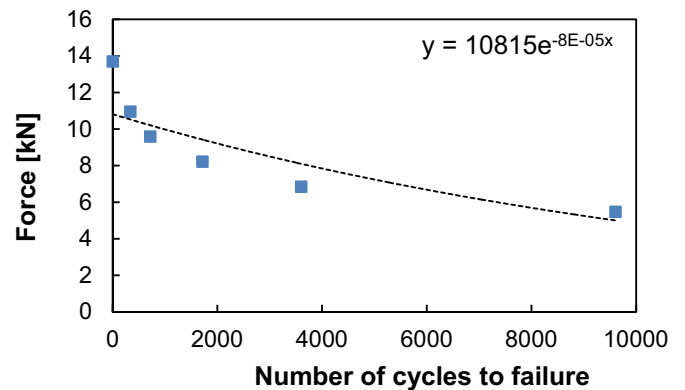


Fig. 9. Low-cycles fatigue behavior for friction stir welded AA2024-T3 joints [set 3-1 (Fig. 5a)]

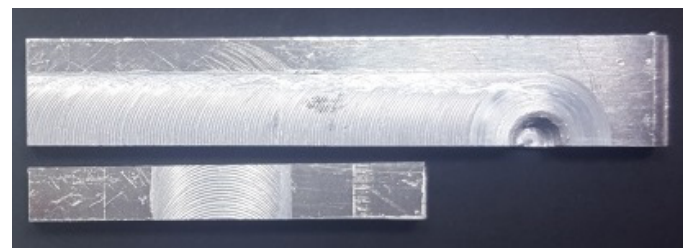


Fig. 10. View of samples prepared for macro and microstructure analysis

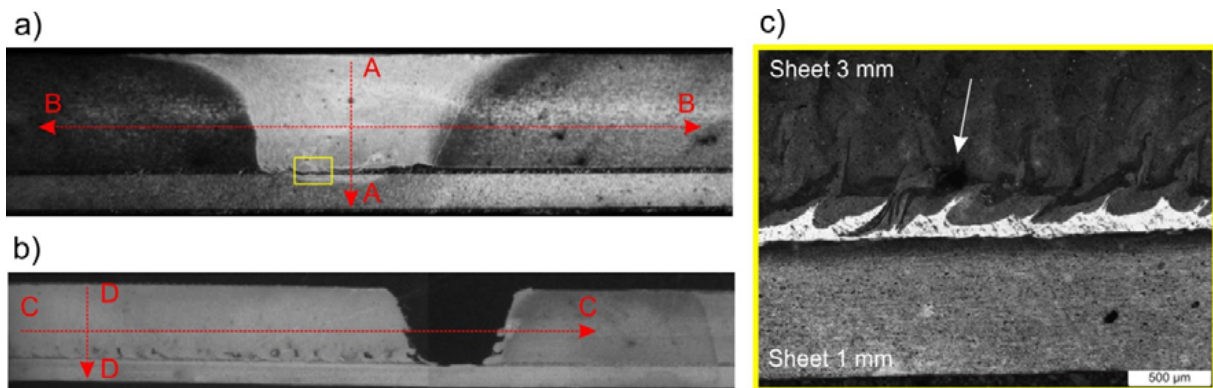


Fig. 11. Macrostructure of weld No. 3 – a) cross-section (perpendicular to the weld axis), b) longitudinal section (along the weld axis), c) cross-section along the weld axis. Visible lines / bands of flow and discontinuities (arrow)

discontinuities are visible as irregular holes / gaps, which are concentrated mainly in the area of deformation lines of very high intensity (Fig. 11c).

The alloy microstructure in the area of welds was observed in their entire cross-section, both transverse and longitudinal. Three areas were identified – from the advancing side, central / middle side and from the retreating side. For all tested samples, the influence of the welding process is most visible in the weld axis (nugget zone). This area is characterized by fine, equiaxed grains and significant fragmentation and globularization of particles strengthening the intermetallic phase Al-Mg-Cu (Fig. 12). In all areas of welds and heat affected zones, the grains have an equiaxial shape, which indicates that recrystallization occurs.

From a microstructural viewpoint, the important process variables are (a) weld temperature and its gradient, (b) weld strain and strain gradient (c) and strain rate. For a given tool, the principal variation will however be in the temperature and strain rate applied. Thus, the joint efficiency is expected to depend strongly on the thermal cycle (peak process temperature, heating and cooling rates) which again is a function of the heat flux in the workpiece during the process [13]. The issue is visible in two cases. Comparing two sets of process parameters 700 rpm and 200 mm/min and 600 rpm and 150 mm/min we can see that the first set generates too high temperature due to high tool revolutions as well as the deformation speed of the material is also too high. As a result, we get a much worse quality connector when the process parameters are slightly lower.

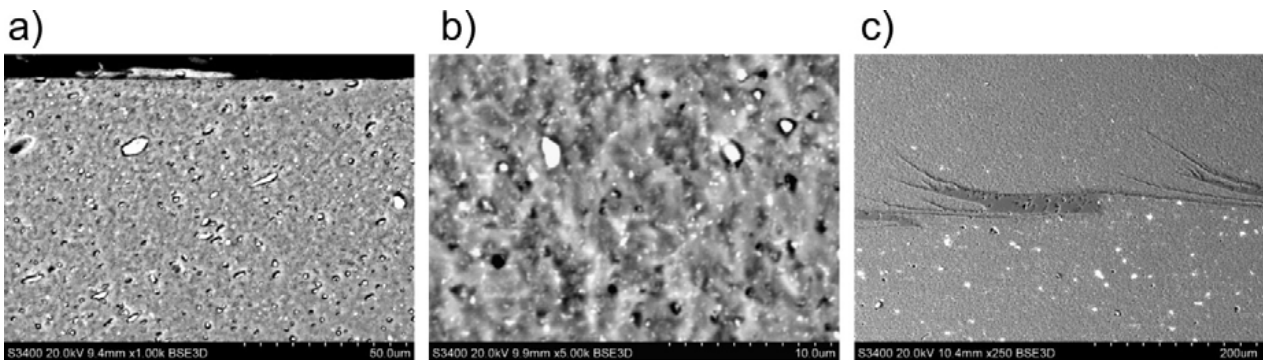


Fig. 12. The microstructure of AA2024-T3 in the weld axis area – a) surface zone, b) middle zone, c) weld bottom zone

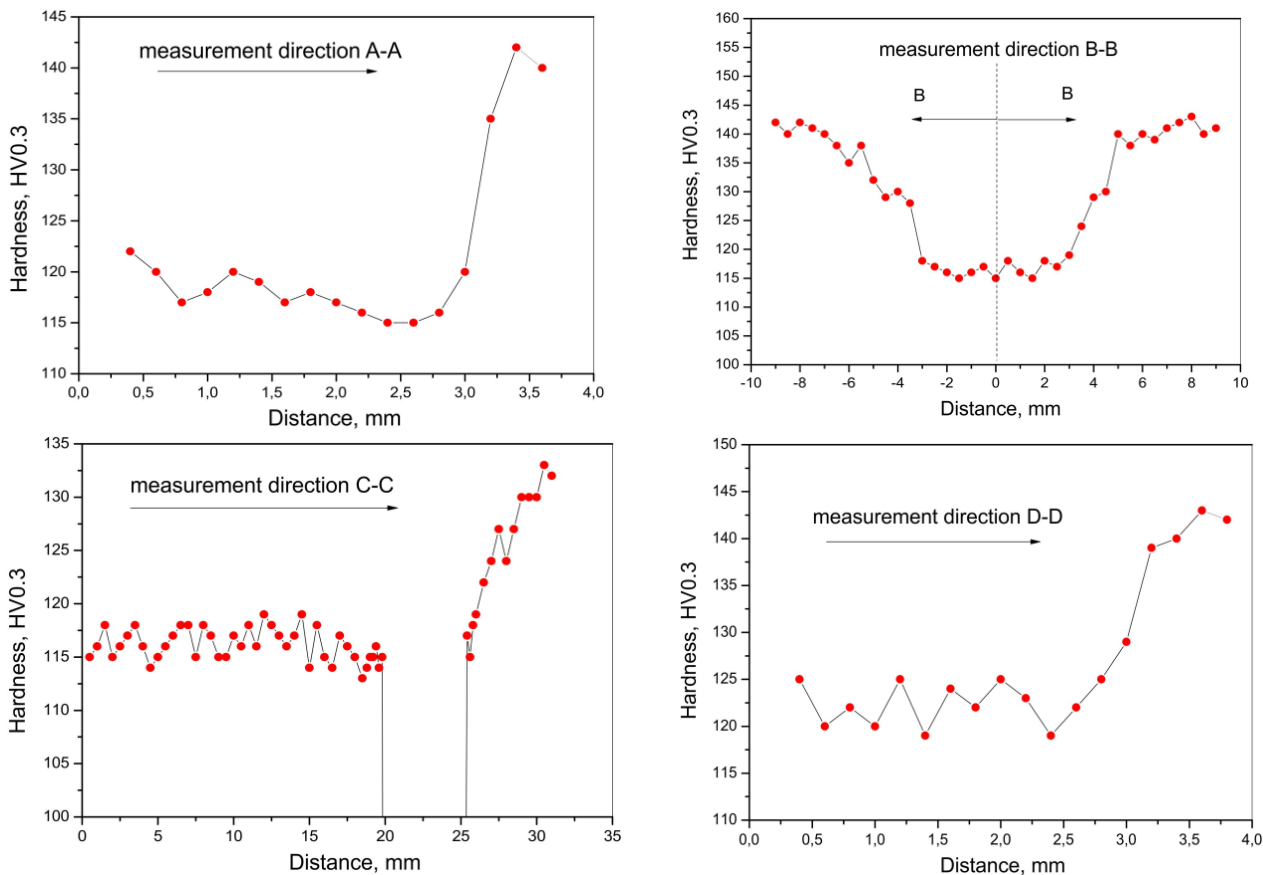


Fig. 13. Microhardness distribution towards A, B, C and D direction

2.4. Micro hardness of FSW joints

The weld micro-hardness was measured by the Vickers HV method at 3N load. The measurements were taken in two perpendicular directions A-A and B-B (cross-section) and C-C and D-D (longitudinal section) – Fig. 11a, b. The measurement results show that for all tested samples the hardness value decreases in the weld area, especially in the central area. In the case of weld No. 3, the change in hardness occurs similarly – continuously and smoothly from the highest value in the sheet area through the lower one in the heat affected zone (HAZ) and the lowest in the weld area. The results of hardness measurements are shown in Fig. 13 and in Table 6.

Depending on the welding parameters, the weakest region in friction stir welded Al alloys [consisting of weld nugget (WN), thermomechanical affected zone (TMAZ), HAZ and parent material (PM)] can be at HAZ, HAZ/TMAZ boundary or in the NZ (nugget zone) itself. To appreciate this difference, the hardness

variations along the transverse weld section of a Al alloy are shown in Fig. 13b. Typically, the weld hardness profile can be classified into either W shape or V shape [14]. In this case, the hardness profile shape adopts the V shape.

3. Manufacture of a landing gear beam of the M28 aircraft by FSW

The final stage of work was the manufacture of the landing gear beam of the M28 aircraft. To this end, a special fastening device has been developed to make the beam (demonstrator). The fastening device was based on technical documentation provided by PZL Mielec. A characteristic feature of the structural element is the need to weld elements of varying geometry and thickness. All elements of the demonstrator are made of AA2024-T3 aluminum alloy. Views of the specially designed fastening devices are shown in Table 7. The whole work was divided into 2 operations, therefore 2 separate instruments were made. The order of work and view of specially designed fastening devices and welding parameters are shown in Table 7. Experimental tests in the laboratory have shown that it is most advantageous to carry out a welding process from the thick plate. The joints are definitely more durable. In addition, the thicker plate from the tool side presses all the elements together more stably during the process, which also simplifies the tooling (less stiffening and pressing elements). Another very important factor is greater process stability of the impact on technological parameters. Performed experiments show that it is possible to obtain high-quality joints in a wide range of parameters. This is an important factor from the point of view of industrial im-

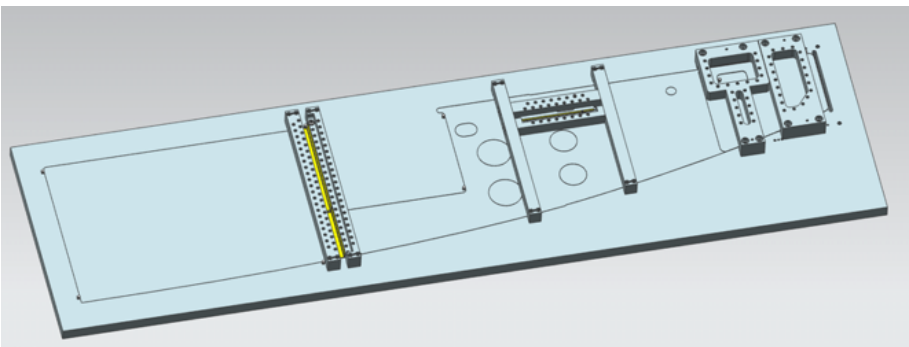
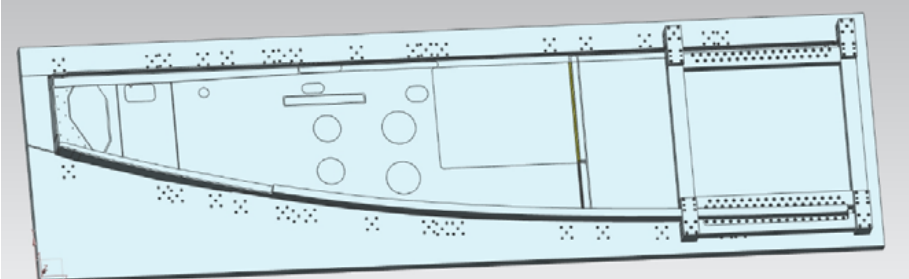
TABLE 6

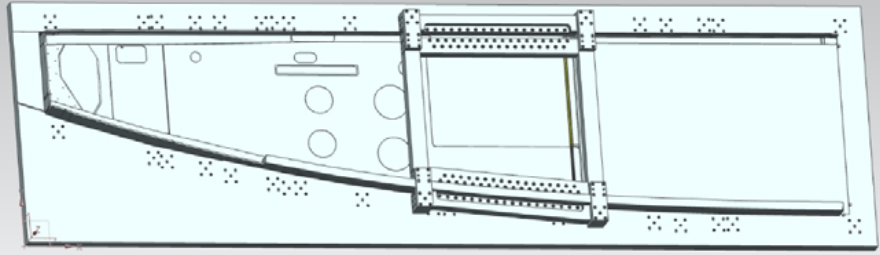
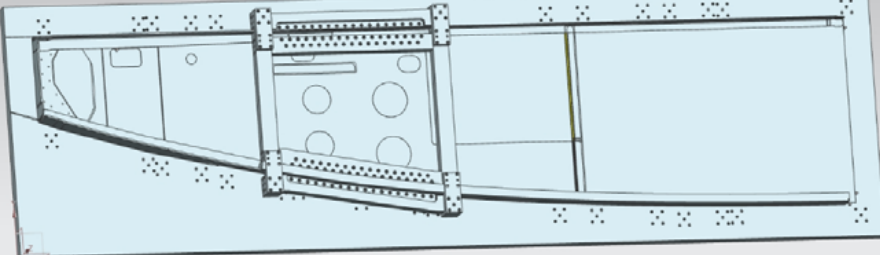
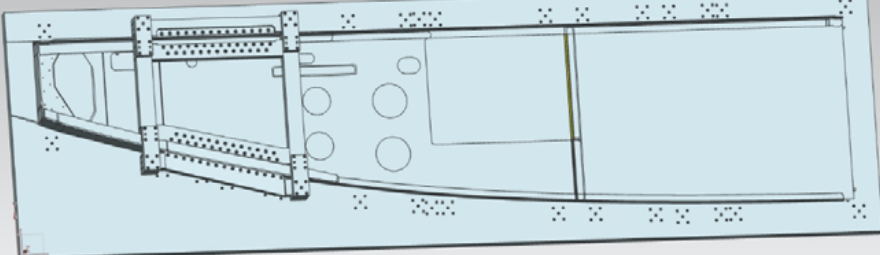
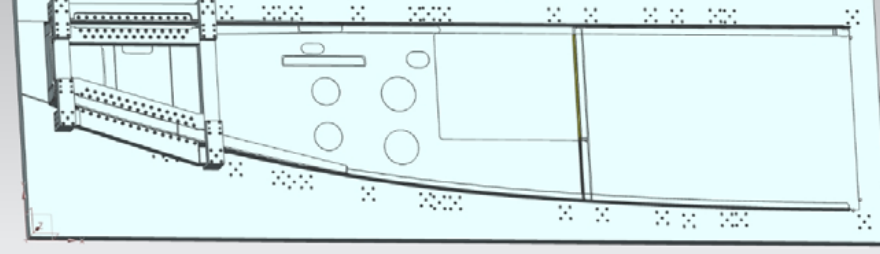
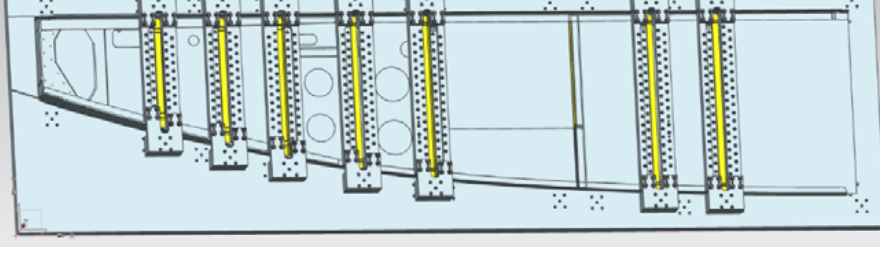
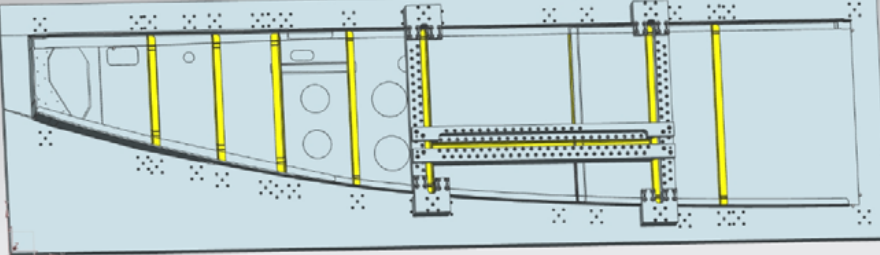
Hardness of AA2024-T3 alloy (sample No. 3) depending on the area on the weld cross-section (average values)

Measurement direction	Hardness HV0.3					
	Face side	Ridge side	Nugget zone	Axis of weld	Heat affected zone	Parent material
Direction A-A	122	140	114			
Direction B-B				115	130	142
Direction C-C				125		132
Direction D-D			116 (sheet 3 mm)			143 (sheet 1 mm)

TABLE 7

View of tooling system for the manufacture of the FSW technology demonstrator

<p>Tooling system 1 for performing operation 1 (steps 1-6) Sheet of 3 mm to 1 mm in thickness</p> <p>Parameters: Tool rotation: 700 rpm Welding speed: 200 mm/min</p>	
<p>Operation 2 Step 2 Sheet of 1,6 mm to 1 mm in thickness</p> <p>Parameters: Tool rotation: 700 rpm Welding speed: 150 mm/min</p>	

<p>Tooling system 2 for performing operation 2, step 1 Sheet 1,6 mm to 1 mm in thickness</p> <p>Parameters: Tool rotation: 700 rpm Welding speed: 150 mm/min</p>	
<p>Operation 2 Step 3 Sheet of 1,6 mm to 1 mm in thickness</p> <p>Parameters: Tool rotation: 700 rpm Welding speed: 150 mm/min</p>	
<p>Operation 2 Step 4 Sheet of 1,6 mm to 1 mm in thickness</p> <p>Parameters: Tool rotation: 700 rpm Welding speed: 150 mm/min</p>	
<p>Operation 2 Step 5 Sheet of 1,6 mm to 1 mm in thickness</p> <p>Parameters: Tool rotation: 700 rpm Welding speed: 150 mm/min</p>	
<p>Operation 2 Steps 6-12 Sheet of 1 mm to 1 mm in thickness</p> <p>Parameters: Tool rotation: 600 rpm Welding speed: 150 mm/min</p>	
<p>Operation 2 Step 13 Sheet of 1 mm to 1 mm in thickness</p> <p>Parameters: Tool rotation: 600 rpm Welding speed: 150 mm/min</p>	

plementation. Welding from the thick plate causes a significant increase in the axial force acting on the tool. This happens as a result of using larger diameter of tools, this affects the use of a suitably rigid technological machine. The technological parameters of the process under industrial conditions should be selected so that the rotational speed of the tool is as low as possible and the welding speed as high as possible, of course in such a way that it is possible to obtain high quality welds without defects. This approach will minimize the formation of too much heat that can adversely affect the strength of the joint and the formation of large deformations of the joined elements. Reduction of the process temperature can also be achieved by blowing cold air into the tool's working area. This should be done carefully so as not to lead to excessive cooling of the joint formation zone.

The production process of the demonstrator was divided into 2 operations. Operation 1 contained a total of 6 steps while operation 2 contained 12 steps. The welding process was carried out using commercial tools dedicated to the FSW process. The FSW process is carried out on CNC machines. Figure 14 shows the adopted CNC machine with used tools. Figure 15 a and b shows a welded demonstrator by FSW.

4. Conclusions

It has been shown that the arrangement of sheet metal is important for the strength of FSW joints. The configuration where the thicker plate is on top is almost 2 times stronger than when the thin plate is on the top. The use of thick sheet metal at the top

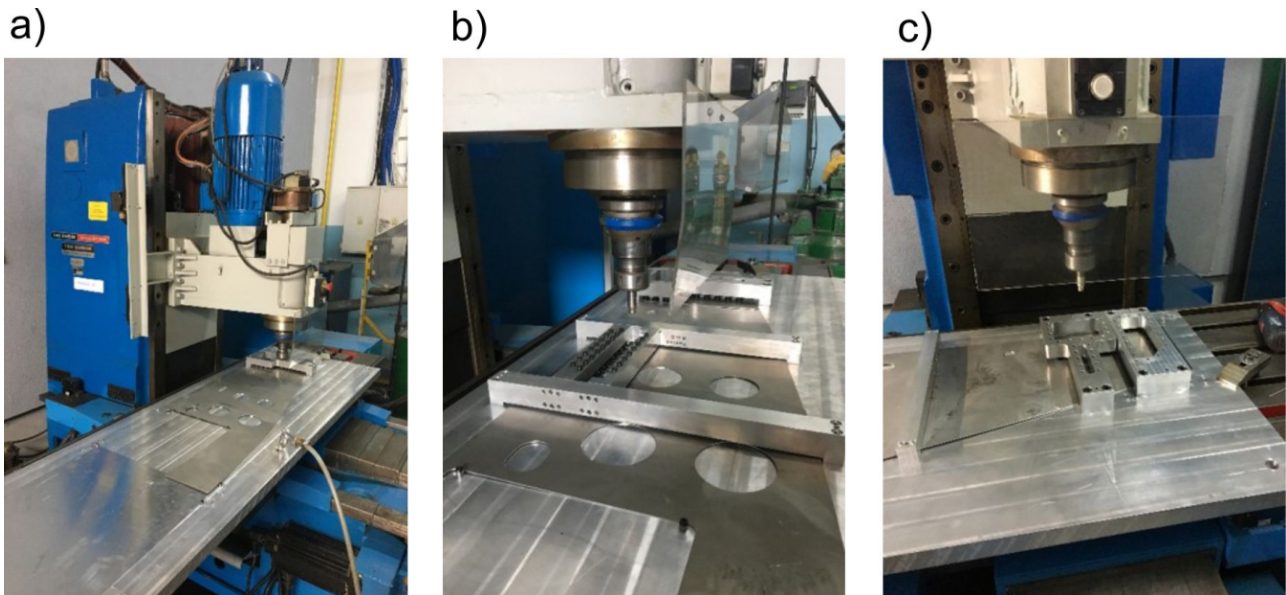


Fig. 14. The CNC machines adopted for FSW process with mounted tools, a) general view, b) and c) close-up view



Fig. 15. View of the welded elements of the M28 aircraft landing gear beam (demonstrator), a) front side, b) back side

of the lap joint is also less sensitive to process parameters. In a large range of parameters we obtain a good joint quality. Joint efficiency of 87% has been obtained for welding using a rotational speed and welding speed of 800 rpm and 250 mm/min. The disadvantage of this arrangement is the decidedly greater axial force during welding and a greater tendency to thermal deformation and residual stress. The microhardness measurement showed that the microhardness in the stir zone is lower compared to the parent material. It can be caused by long-lasting high temperature and grain re-growth. Low-cycle fatigue tests have shown that fatigue strength is largely influenced by joint geometry. Crack propagation was initiated in a thicker plate.

Within the presented case study it has been shown that the geometry of the FSW joint is of great importance for its strength. It has been shown that the welding joint from the thicker side has definitely greater strength in a wide range of technological parameters. This case study demonstrated the ability to join highly complex geometries, using FSW technology which was shown on the presented aviation structure element. Using the FSW technology, it was possible to eliminate riveted joints, which significantly reduces the time of manufacturing parts. It is also important to highlight the applicability of such a welding approach to a large range of products, not only in aviation but also in other industries, where large thermal variation may affect the welding process.

Acknowledgements

The work was carried out in the framework of SAT-AM project AIRFRAME ITD. Grant Agreement No: CS2-AIR-GAM-2014-2015-01 (annex III), Topic: JTI-CS2-2015-CPW02-AIR-02-07 Proposal Number/ Acronym: 699757/SAT-AM

REFERENCES

- [1] W.M. Thomas, Nicholas, both of Haverhill; James C. Needham, Saffron Walden; Michael G. Murch, Herts; Peter Temple-Smith, Cambridge; Christopher J. Dawes, Cambs, all of United Kingdom, s. 19, 1995.
- [2] G.K. Padhy, C.S. Wu, S. Gao, Friction stir based welding and processing technologies - processes, parameters, microstructures and applications: A review, *Journal of Materials Science & Technology* **34**, 1, 1-38, (2018), doi: 10.1016/j.jmst.2017.11.029.
- [3] M.K. Kulekci, U. Esmel, B. Buldum, Critical analysis of friction stir-based manufacturing processes, *The International Journal of Advanced Manufacturing Technology* **85**, 5-8, 1687-1712, (2016), doi: 10.1007/s00170-015-8071-5.
- [4] W.J. Arbegast, A flow-partitioned deformation zone model for defect formation during friction stir welding, *Scripta Materialia* **58**, 5, 372-376 (2008), doi: 10.1016/j.scriptamat.2007.10.031.
- [5] S. Bag, D. Yaduwanshi, S. Pal, Heat transfer and material flow in friction stir welding, w *Advances in Friction-Stir Welding and Processing*, Elsevier, 21-63 (2014).
- [6] H. Liu, Y. Hu, Y. Peng, C. Dou, Z. Wang, The effect of interface defect on mechanical properties and its formation mechanism in friction stir lap welded joints of aluminum alloys, *Journal of Materials Processing Technology* **238**, 244-254 (2016), doi: 10.1016/j.jmatprotec.2016.06.029.
- [7] R.K. Bhushan, D. Sharma, Green welding for various similar and dissimilar metals and alloys: present status and future possibilities, *Adv Compos Hybrid Mater.* **2**, 3, 389-406 (2019), doi: 10.1007/s42114-019-00094-8.
- [8] H. Doude, J. Schneider, B. Patton, S. Stafford, T. Waters, C. Varner, Optimizing weld quality of a friction stir welded aluminum alloy, *Journal of Materials Processing Technology* **222**, 188-196 (2015), doi: 10.1016/j.jmatprotec.2015.01.019.
- [9] R.A. Gite, P.K. Loharkar, R. Shimpi, Friction stir welding parameters and application: A review, *Materials Today: Proceedings*, 2019, doi: 10.1016/j.matpr.2019.07.613.
- [10] Y.N. Zhang, X. Cao, S. Larose, P. Wanjara, Review of tools for friction stir welding and processing, *Canadian Metallurgical Quarterly* **51**, 3, 250-261 (2012), doi: 10.1179/1879139512Y.0000000015.
- [11] R. Rai, A. De, H.K.D.H. Bhadeshia, T. DebRoy, Review: friction stir welding tools, *Science and Technology of Welding and Joining* **16**, 4, 325-342 (2013), doi: 10.1179/1362171811y.0000000023.
- [12] B. Farahmand, G. Bockrath, J. Glassco, *Fatigue and Fracture Mechanics of High Risk Parts*. Boston, MA: Springer US, 1997.
- [13] O.S. Salih, H. Ou, W. Sun, D.G. McCartney, A review of friction stir welding of aluminium matrix composites, *Materials & Design* **86**, 61-71 (2015), doi: 10.1016/j.matdes.2015.07.071.
- [14] P.S. De, R.S. Mishra, Friction stir welding of precipitation strengthened aluminium alloys: scope and challenges, *Science and Technology of Welding and Joining* **16**, 4, 343-347 (2011), doi: 10.1179/1362171811Y.0000000020.